

SUPPLEMENTAL MATERIAL

Transgenic mice for cGMP imaging

Martin Thunemann^{1,*}, Lai Wen^{1,*}, Matthias Hillenbrand¹, Angelos Vachaviolos¹, Susanne Feil¹, Thomas Ott², Xiaoxing Han³, Dai Fukumura³, Rakesh K. Jain³, Michael Russwurm⁴, Cor de Wit⁵ & Robert Feil^{1#}

¹ Interfakultäres Institut für Biochemie, Universität Tübingen, Germany

² IZKF - Transgene Tiere, Universität Tübingen, Germany

³ Edwin L. Steele Laboratory for Tumor Biology, Department of Radiation Oncology, Massachusetts General Hospital and Harvard Medical School, Boston, Massachusetts, USA

⁴ Institut für Pharmakologie und Toxikologie, Universität Bochum, Germany

⁵ Institut für Physiologie, Universität zu Lübeck, Germany

* These authors contributed equally

#Corresponding author:

Robert Feil

Interfakultäres Institut für Biochemie

Universität Tübingen

Hoppe-Seyler-Str. 4

72076 Tübingen, Germany

Tel. +49-7071-29 73350

Fax +49-7071-29 3332

E-mail: robert.feil@uni-tuebingen.de

Methods

Animals

Mice were housed in a conventional mouse facility at 22°C and 50-60% humidity in a 12h/12h light/dark cycle with free access to standard rodent chow and tap water. Adult male and female mice were used for experiments. The cGi500 transgenic mice were heterozygous for the transgene. SM22-cGi500 mice were on a mixed B6D2/C57BL6N or C57BL/6N genetic background, and R26-CAG-cGi500(L1) mice were on a mixed 129Sv/C57BL6N genetic background. Animal procedures were reviewed and approved by the Regierungspräsidium Tübingen and the local authorities in Lübeck and Boston in compliance with the humane care and use of laboratory animals.

Generation of SM22-cGi500 Mice

To generate the plasmid pSM445-cGi500, the CMV promoter in pMGSV1¹ was replaced by a 445-bp fragment of the murine SM22 α promoter (SM445),² followed by insertion of the cGi500 encoding sequence³ between the rabbit β -globin intron and two polyadenylation signals from the rabbit β -globin gene and the SV40 early region. To generate transgenic mice, the BsrBI-digested 4.9-kb fragment of pSM445-cGi500 carrying the transgene (see also Online Figure IA) was microinjected at a concentration of 2 ng/ μ L into fertilized B6D2F1 oocytes. Founder mice carrying the transgene were identified by PCR analysis of genomic tail DNA with the primers cGi-fwd (5'-GTCACCTCGTGAAGACTCG) and cGi500-rev (5'-TGCTCACCATATATTTTGCC), which amplify a 244-bp product of the transgene. PCR-positive SM22-cGi500 mice were backcrossed to C57BL/6N mice and screened for sensor expression by Western blot analysis of smooth muscle-rich tissues with a rabbit polyclonal antibody against EGFP (ab290, Abcam, Cambridge, MA, USA). GAPDH was used as a loading control (anti-GAPDH; #2118, Cell Signaling, Danvers, MA, USA). Out of 11 analyzed founder lines, one [B6;B6D2-Tg(SM445-cGi500)5Feil] showed strong sensor expression in smooth muscle and was suitable for cGMP imaging experiments.

For immunofluorescence staining of primary smooth muscle cells, cells were fixed for 25 min at 37°C in 4% formaldehyde/4% sucrose. After blocking of non-specific binding with 10% normal goat serum/10% BSA, cells were stained with mouse monoclonal anti-EGFP (sc-81045, Santa Cruz, Santa Cruz, CA, USA) and rabbit polyclonal anti-SM22 α (gift from Mario Gimona) followed by Alexa 488- or Alexa 594-coupled secondary antibodies. Nuclei were stained with 1 μ g/ μ L Hoechst 33258 (Sigma-Aldrich Chemie GmbH, München, Germany).

Generation of R26-CAG-cGi500 Knock-in Mice

To generate the targeting vector pR26-CAG-cGi500(L2), the mG sequence of pRosa26-mT/mG⁴ (Addgene plasmid 17787) was replaced by the cGi500 encoding sequence.³ Details of plasmid construction are available on request. The targeting strategy was based on the knock-in into the ROSA26 locus of a CAG promoter-driven Cre-activatable cGi500 transgene (see also Online Figure II). Gene targeting was performed as described.⁵ Briefly, 42 μ g of KpnI-linearized pR26-CAG-cGi500(L2) were electroporated into R1 ES cells (genetic background: 129/Sv x 129/Sv-CP),⁶ and after 8 days of selection with 300 μ g/mL G418, 200 clones were isolated and expanded. Three correctly targeted ES cell clones carrying the Cre-activatable "L2 allele" were identified by Southern blot analysis of EcoRV-digested genomic DNA with a 5' probe that binds to the ROSA26 promoter region.⁷ Targeted R26-CAG-cGi500(L2) ES cells were transiently transfected with a Cre-expressing plasmid (pIC-Cre)⁸ to generate ES cells with the 'excised' R26-CAG-cGi500(L1) allele. ES cell clones were isolated and subjected to Southern blot analysis as described before as well as to fluorescence microscopy to proof excision of mT and activation of cGi500 expression. Out of 96 clones

analyzed 32 were positive for the Cre-excised “L1 allele”. R26-CAG-cGi500(L2) and R26-CAG-cGi500(L1) ES cells carrying the silenced but Cre-activatable “L2 allele” and the Cre-activated “L1 allele” of the cGi500 transgene, respectively (see also Online Figure II), were injected into 3.5 dpc C57BL/6N blastocysts to generate chimeric mice. Male chimeras were mated to C57BL/6N females to obtain heterozygous R26-CAG-cGi500(L2) mice [B6;129-Gt(ROSA26)Sor^{tm1(ACTB-tdTomato,-cGi500)Feil}] or R26-CAG-cGi500(L1) mice [B6;129-Gt(ROSA26)Sor^{tm1.1(ACTB-cGi500)Feil}] on a mixed 129Sv/C57BL6N genetic background. Mice were further backcrossed to C57BL/6N animals. Germline transmission of the targeted alleles was verified by Southern blot analysis of tail DNA. PCR-based genotyping of ear biopsies was done with primers ROSA10 (5'-CTCTGCTGCCTCCTGGCTTCT), ROSA11 (5'-CGAGGCGGATCACAAGCAATA), and ROSA4 (5'-TCAATGGGCGGGGGTCGTT).⁹ ROSA10 and ROSA11 amplify a 330-bp fragment of the wild-type ROSA26 locus, while ROSA10 and ROSA4 amplify a 250-bp fragment of the R26-CAG-cGi500(L2) or R26-CAG-cGi500(L1) allele (see also Online Figure IIA).

For the analysis of cGi500 fluorescence in organs, mice were anesthetized and sacrificed by cervical dislocation. Organs were isolated in ice-cold PBS and whole-mounts were observed with a fluorescence stereo microscope with EGFP filter set (Discovery, Carl Zeiss Microscopy GmbH, Göttingen, Germany). Then, organs were further processed for sectioning; tissues were fixed in 4% paraformaldehyde in PBS at 4°C overnight, cryoprotected in 30% sucrose at 4°C overnight, embedded in O.C.T. compound (Sakura Finetek Germany GmbH, Staufen, Germany), and frozen in 2-methyl butane at -80°C. 10-µm sections were mounted on SuperFrostPlus slides (Carl Roth GmbH, Karlsruhe, Germany). After drying at room temperature and rehydration in PBS, samples were washed 3 times with PBS-T (0.25% Triton X-100 in PBS), mounted with Shandon ImmuMount (ThermoFisher HealthCare, Houston, TX, USA) and observed under a fluorescence microscope with YFP filter set.

FRET Measurements in Primary Cells and Isolated Tissues

Smooth muscle cells were isolated by enzymatic digestion and FRET imaging of cultured cells and tissues was performed with an epifluorescence-based setup as previously described.^{5,10} Briefly, smooth muscle-rich tissues were isolated from 2-5 transgenic mice (5- to 10-week-old) in ice-cold PBS. For VSMCs, surrounding fat and connective tissue were removed from the aorta; for CSMCs, the smooth muscle layer was separated and cleaned from fat and blood vessels; for BSMCs, the inner epithelium and surrounding fat were removed. Then, tissues were cut into 5-mm pieces and incubated at 37°C for 45 min with papain (0.7 mg/mL), followed by 10-15 min with collagenase (1 mg/mL) and hyaluronidase (1 mg/mL); tissues were dissociated by pipetting through a 1000-µL pipette tip. Cells (viability >90% as measured by trypan blue exclusion) were suspended in culture medium (DMEM with 4.5 g/L glucose, 100 U/mL Penicillin, 100 µg/mL Streptomycin, 10% fetal bovine serum) and plated into 12-well plates equipped with glass coverslips (6x10⁴ VSMCs, 4x10⁴ BSMCs, 3x10⁴ CSMCs per well). Cells were grown at 37°C and 5% CO₂. After 3 days, medium was exchanged. Cells were grown for additional 1-4 days in culture medium before they were serum-starved in culture medium without serum for 24-48 h prior to imaging experiments. These cell cultures contained >90% SM22α-positive cells. Fibroblasts were obtained from adult mouse tail tissue. Tail-tips were skinned and minced and then placed into wells of a 12-well plate containing culture medium and glass coverslips. The cells were grown at 37°C and 5% CO₂ for 7-10 days before analysis.

The imaging setup was composed of an Axiovert 200 inverted microscope with EC Plan NeoFluar 10x/0.30 air or 40x/1.30 oil objectives and optional 1.6x Optovar magnification (Carl Zeiss Microscopy GmbH, Göttingen, Germany), a light source with excitation filter switching device (Oligochrome, TILL Photonics GmbH, Gräfelfing, Germany), a DualView beam splitter with 516 nm dichroic mirror and CFP and YFP emission filters (480/30 nm and 535/40 nm) (Photometrics, Tucson, AZ, USA), and a EM-CCD digital camera (Retiga 2000R, QImaging, Surrey, BC, Canada). To set up the field of view, cGi500 fluorescence was

observed through an YFP filter set (excitation filter 497/16 nm, 516 nm dichroic mirror, emission filter 535/22 nm). For FRET measurements, a CFP excitation filter (445/20 nm) was used together with a 470 nm dichroic mirror and the beam splitter device. The system was operated by Live Acquisition software (TILL Photonics GmbH) and images were recorded with arivis Browser 2D (arivis GmbH, Berlin, Germany).

For cGMP imaging of primary cells, cells were grown on glass coverslips. The coverslips were mounted into a custom-built superfusion imaging chamber, so that they define the chamber bottom. For cGMP imaging of retinal vessels, an acutely isolated retina was immobilized on a MF membrane filter (Millipore) with a 5x2.5 mm hole; the filter was fixed with silicon grease on a coverslip serving as chamber bottom, and the inner layer of the retina faced towards the chamber bottom. Samples were superfused with imaging buffer (in mM: NaCl 140, KCl 5, MgSO₄ 1.2, CaCl₂ 2.5, Glucose 5, HEPES 5, pH 7.4) at room temperature using a pump (Pharmacia P-500, GE Healthcare Europe GmbH, Freiburg, Germany) set to 1 mL/min and two injection valves (Pharmacia V-7, GE Healthcare) with 2-mL and 20-mL sample loops connected in series to apply test compounds (diluted in imaging buffer). The solution in the imaging chamber was continuously removed by aspiration.

cGMP Measurements by ELISA

Primary smooth muscle cells were grown in 6-well plates and serum-starved for 24 h. Cells were kept at room temperature in imaging buffer (2 mL/well) for 10 min. At t=10 min, the buffer was replaced with imaging buffer containing 200 nM DEA/NO for 2 min. At t=12 min, cells were washed once with imaging buffer and incubated in imaging buffer for another 3 min (t=15 min). At t=10 min, 12 min, and 15 min, aliquots of the cells were lysed in ice-cold ethanol (700 µL/well). For each time point, cells from 2 wells were pooled. Cells were scraped from the dish with a blue pipette tip, and lysates were centrifuged for 10 min at 20,000 g and 4°C. The ethanol from the cGMP-containing supernatants was evaporated in a vacuum concentrator. The resulting pellet was dissolved in EIA buffer, and cGMP was determined without acetylation with the Cyclic GMP EIA Kit (Cayman Chemical) according to manufacturer's instructions. To estimate the intracellular cGMP concentration, cell numbers per 6-well were determined from trypsinized culture replicates in a Neubauer chamber, and the cell volume was considered to be 1 pL.¹¹

Expression Analysis by RT-PCR

Total RNA was isolated from serum-starved smooth muscle cells using phenol- and guanidine isothiocyanate-containing PEQGold RNAPure according to manufacturer's instructions. The RNA pellet was dissolved in DEPC-treated water and adjusted to 0.1 µg/µL. Semi-quantitative RT-PCR was performed as described¹ with primers for soluble guanylyl cyclase (*Gucy1a3* or *Gucy1b3* encoding the $\alpha 1$ or $\beta 1$ subunit, respectively) and particulate guanylyl cyclases (*Npr1* or *Npr2* encoding GC-A or GC-B, respectively)¹² and, as internal control, for *Gapdh*.¹³

Intravital FRET Measurements in the Cremaster Microcirculation

Preparation of the cremaster muscle of mice for intravital microscopy was performed as previously described.¹⁴ The skeletal muscle was carefully removed from selected arterioles to reduce fluorescence signals from non-target tissue. The imaging setup was composed of an upright microscope (Axioskop 2 FS, Carl Zeiss Microscopy GmbH) equipped with a water immersion objective (Achromplan 40x/1.75w) which allowed conventional microscopy to identify and select arterioles for examination that exhibited intact blood flow. FRET measurements were performed using dichroic mirrors and filters as described above, as well as a polychromatic light source (Polychrome V, TILL Photonics) set to 420 nm in this setup. A camera (Andor iXon 885 EM-CCD, Andor Technology, Belfast, Northern Ireland) was

connected to the beam splitter (DualView, Photometrics) for image recording. The tissue was superfused at a rate of 8 ml/min with warmed (34°C) salt solution (in mM: NaCl 118.4, NaHCO₃ 20, KCl 3.8, CaCl₂ 2.5, KH₂PO₄ 1.2, MgSO₄ 1.2) gassed with 5% CO₂ and 95% N₂ to yield a pCO₂ of ~40 mmHg and a pH of 7.4. The pO₂ at the surface of the tissue was 20-30 mmHg due to contamination with ambient air. Adenosine (1 mM) was dissolved in water, DEA/NO (1 mM) in NaOH (10 mM) and both were added to the superfusion solution using a roller pump to achieve a dilution of 1:100 and thus a final concentration of 10 μM on the tissue.

Intravital FRET Measurements in the Dorsal Skinfold Chamber

Dorsal skinfold chambers were implanted into adult mice as described.¹⁵ Mice were allowed to recover from surgery for at least 14 days. Anesthetized mice were provided with a tail vein catheter for drug injection and imaged using a custom-built setup for multi-photon FRET microscopy of dorsal skinfold chambers. Fluorescent signal was excited by a Spectra Physics MaiTai Ti:Sapphire laser providing 100 fs pulses at 80 MHz repetition rate and 850 nm wavelength. Beam scanning and image acquisition were performed with an Olympus Fluoview FV300 scanning system interfaced with an Olympus BX51WI upright microscope. The objective was an Olympus XLUMPFL20x W/IR water immersion lens (20x, 0.95 N.A.). The fluorescent signal from CFP and YFP was first separated from the excitation beam by a dichroic mirror (750DCSPXR, Chroma), then separated into CFP and YFP channels by another dichroic mirror (505DCLP, Chroma) and two band pass filters (FF01-483/32-25 and FF01-542/27-25, Semrock) and detected by two separate photomultiplier tubes (HC125-02, Hamamatsu). The resolution of the images was 512 x 512 for a total field of view of 600x600 μm. The excitation laser power was 400 mw before the scanner and 36 mw at the sample surface. The separation between two consecutive images in a time series was 5 or 10 s. After baseline acquisition, either 100 μL saline or 100 μL DEA/NO (0.1 mM or 1 mM diluted in saline) were injected within 5-10 s through the catheter.

To evaluate FRET ratio signals in the vessel wall it was necessary to account for dynamic changes in vessel diameter, which happened particularly during NO-induced vasodilation. Therefore, image segmentation according to brightness was performed following the strategy of Zhang and colleagues.¹⁶ Images in the CFP channel were used to define a dynamic binary mask with a threshold that was manually set. Within this mask, all bright structures (e.g., the vessel wall) receive the value “1”, while all dark structures (e.g., the vessel lumen) that fall below the threshold are set to be “not a number” (NaN). Then, this dynamic mask was multiplied with the originally recorded CFP and YFP time-lapse images. In the resulting time-lapse images, regions of interest were defined that were large enough to account for movements of the vessel walls throughout the experiment. Average intensities of a region of interest were calculated without background correction for the evaluation of FRET data (see below). Vessel diameters were estimated from time-lapse images in the CFP channel by measuring the distance between two adjacent vessel walls. FRET ratio signals and vessel diameters were normalized to the baseline period recorded at the beginning of each experiment.

Evaluation of FRET Data

Offline analysis was performed with arivis Browser 2D software (arivis GmbH, Berlin) or ImageJ¹⁷; for further data evaluation Microsoft Excel (Microsoft Corp., Redmond, WA, USA) and Microcal Origin (OriginLab Corp., Northampton, MA, USA) were used. Background-corrected F₄₈₀ and F₅₃₅ signals were used to calculate the F₄₈₀/F₅₃₅ ratio R. $\Delta F_{480}/F_{480}$, $\Delta F_{535}/F_{535}$, and $\Delta R/R$ traces were obtained by normalization to the baseline recorded for 2-5 min at the beginning of each experiment. For $\Delta R/R$ peak area estimation, the Peak Analyzer Module of Origin was used; single cell traces were corrected for baseline drifts by subtracting a linear baseline, and peak borders were manually defined. For EC₅₀ estimation, a dose-

response function was fitted to the mean peak areas, yielding A_{\min} , A_{\max} , $\log(EC_{50})$ and the Hill constant. For normalization, averaged mean peak areas were divided by A_{\max} , and error bars were calculated by $[\text{err}(\text{area})+\text{err}(A_{\max})]/A_{\max}$.

Statistics

To compare DEA/NO dose-response curves, a two-tailed student's t-test was performed. For PDE inhibitor studies with triple DEA/NO stimulation, a ranked ANOVA with repeated measurements was performed on peak areas using SigmaPlot 11 (Systat Software, Inc., Chicago, IL, USA) and Tukey's post-hoc test to compare individual DEA/NO stimulations. P values <0.05 were considered to be significant.

Supplementary References

1. Feil R, Brocard J, Mascrez B, LeMeur M, Metzger D, Chambon P. Ligand-activated site-specific recombination in mice. *Proc Natl Acad Sci U S A*. 1996;93:10887-10890.
2. Li L, Miano JM, Mercer B, Olson EN. Expression of the SM22alpha promoter in transgenic mice provides evidence for distinct transcriptional regulatory programs in vascular and visceral smooth muscle cells. *J. Cell Biol*. 1996;132:849-859.
3. Russwurm M, Mullershausen F, Friebe A, Jager R, Russwurm C, Koesling D. Design of fluorescence resonance energy transfer (FRET)-based cGMP indicators: a systematic approach. *Biochem J*. 2007;407:69-77.
4. Muzumdar MD, Tasic B, Miyamichi K, Li L, Luo L. A global double-fluorescent Cre reporter mouse. *Genesis*. 2007;45:593-605.
5. Kuhbandner S, Brummer S, Metzger D, Chambon P, Hofmann F, Feil R. Temporally controlled somatic mutagenesis in smooth muscle. *Genesis*. 2000;28:15-22.
6. Nagy A, Rossant J, Nagy R, Abramow-Newerly W, Roder JC. Derivation of completely cell culture-derived mice from early-passage embryonic stem cells. *Proc Natl Acad Sci U S A*. 1993;90:8424-8428.
7. Hitz C, Wurst W, Kuhn R. Conditional brain-specific knockdown of MAPK using Cre/loxP regulated RNA interference. *Nucleic Acids Res*. 2007;35:e90.
8. Gu H, Zou YR, Rajewsky K. Independent control of immunoglobulin switch recombination at individual switch regions evidenced through Cre-loxP-mediated gene targeting. *Cell*. 1993;73:1155-1164.
9. Zong H, Espinosa JS, Su HH, Muzumdar MD, Luo L. Mosaic analysis with double markers in mice. *Cell*. 2005;121:479-492.
10. Thunemann M, Fomin N, Krawutschke C, Russwurm M, Feil R. Visualization of cGMP with cGi biosensors. *Methods Mol Biol*. 2013;1020:89-120.
11. Hevia D, Rodriguez-Garcia A, Alonso-Gervós M, Quirós-González I, Cimadevilla HM, Gómez-Cordovés C, Sainz RM, Mayo JC. Cell volume and geometric parameters determination in living cells using confocal microscopy and 3D reconstruction. 2011; doi: 10.1038/protex.2011.272.
12. Schmidt H, Stonkute A, Juttner R, Schaffer S, Buttgerit J, Feil R, Hofmann F, Rathjen FG. The receptor guanylyl cyclase Npr2 is essential for sensory axon bifurcation within the spinal cord. *J Cell Biol*. 2007;179:331-340.

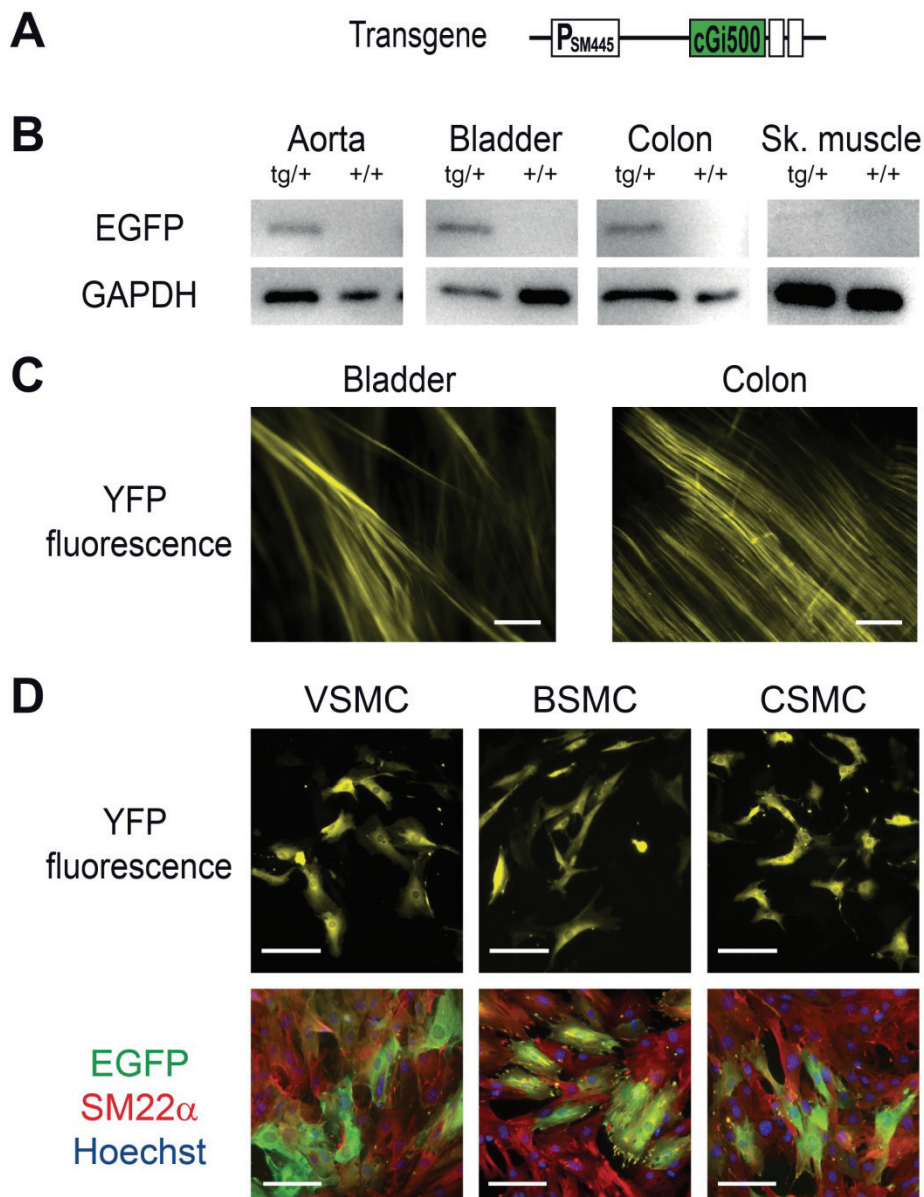
13. Davies E, Omer S, Buckingham JC, Morris JF, Christian HC. Expression and externalization of annexin 1 in the adrenal gland: structure and function of the adrenal gland in annexin 1-null mutant mice. *Endocrinology*. 2007;148:1030-1038.
14. Wolfle SE, Schmidt VJ, Hoyer J, Kohler R, de Wit C. Prominent role of KCa3.1 in endothelium-derived hyperpolarizing factor-type dilations and conducted responses in the microcirculation in vivo. *Cardiovasc Res*. 2009;82:476-483.
15. Jain RK, Munn LL, Fukumura D. Transparent window models and intravital microscopy: Imaging gene expression, physiological function and therapeutic effects in tumors. In: Teicher BA, ed. *Tumor models in cancer research*. Totowa: Humana Press Inc.; 2011: 641-679.
16. Zhang J, Chen L, Raina H, Blaustein MP, Wier WG. In vivo assessment of artery smooth muscle $[Ca^{2+}]_i$ and MLCK activation in FRET-based biosensor mice. *Am J Physiol Heart Circ Physiol*. 2010;299:H946-H956.
17. Rasband WS. ImageJ. 1997-2012; <http://imagej.nih.gov/ij/>.

Online Movies

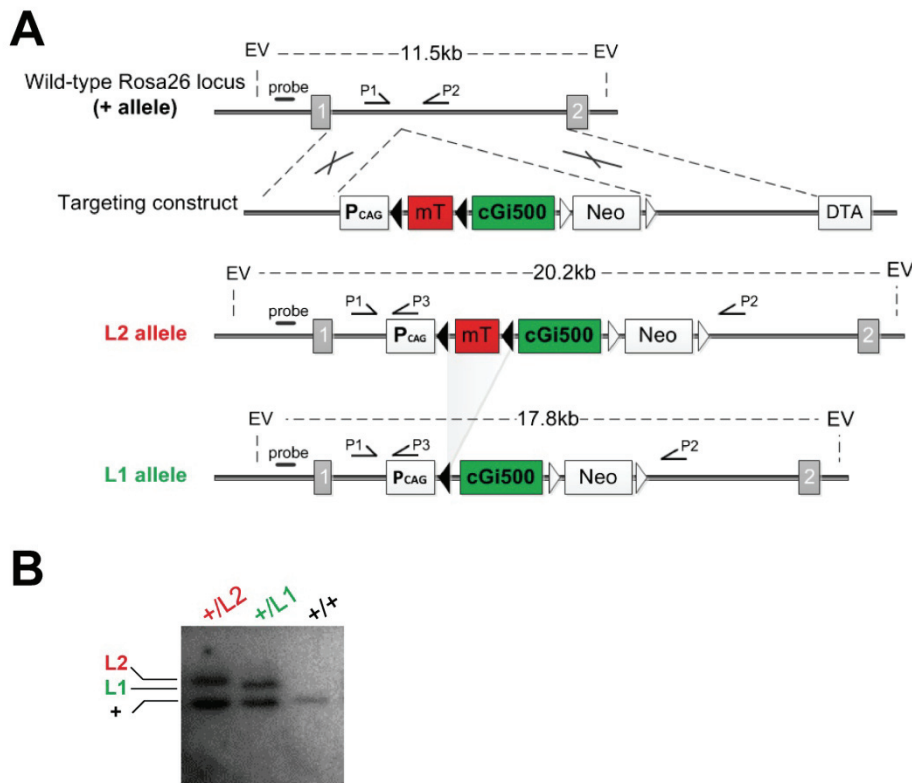
Online Movie I. cGMP imaging in a cremaster arteriole of an anesthetized R26-CAG-cGi500(L1) mouse. This movie shows the FRET ratio signal (reflecting the intracellular cGMP concentration) that was recorded by epifluorescence microscopy during the experiment shown in Figure 5. Upon repeated superfusion of 10 μ M DEA/NO (indicated in the top right corner) robust cGMP transients were detected in this vessel.

Online Movie II. NO-induced vasodilation observed by multi-photon microscopy in a dorsal skinfold chamber of an anesthetized R26-CAG-cGi500(L1) mouse. This movie was recorded during the experiment shown in Figure 6C and 6D. Three i.v. injections (100 μ L) of 0.1 mM DEA/NO were followed by two injections (100 μ L) of 1 mM DEA/NO (indicated in the top right corner). The lower dose of DEA/NO resulted in transient vasorelaxations, whereas the higher dose induced a sustained dilation. Note that the movie shows sensor fluorescence recorded in the CFP channel, but not the FRET ratio signal.

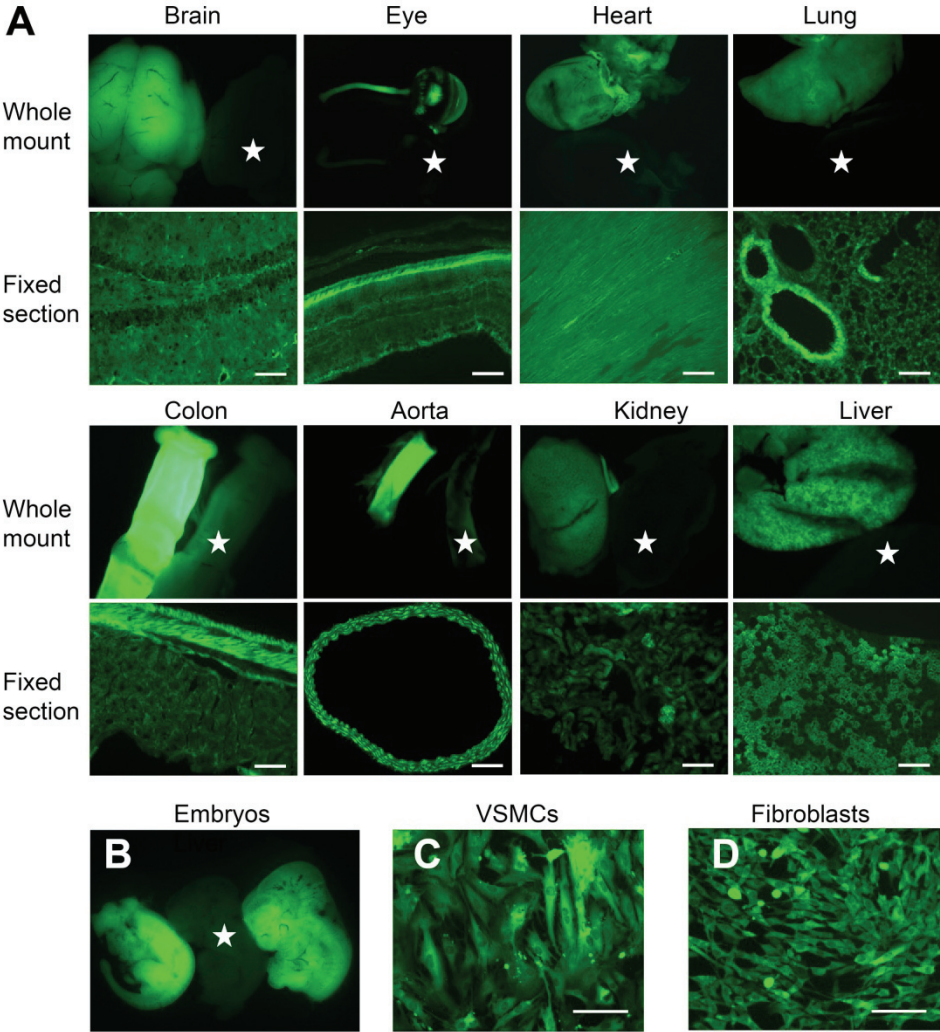
Online Figures



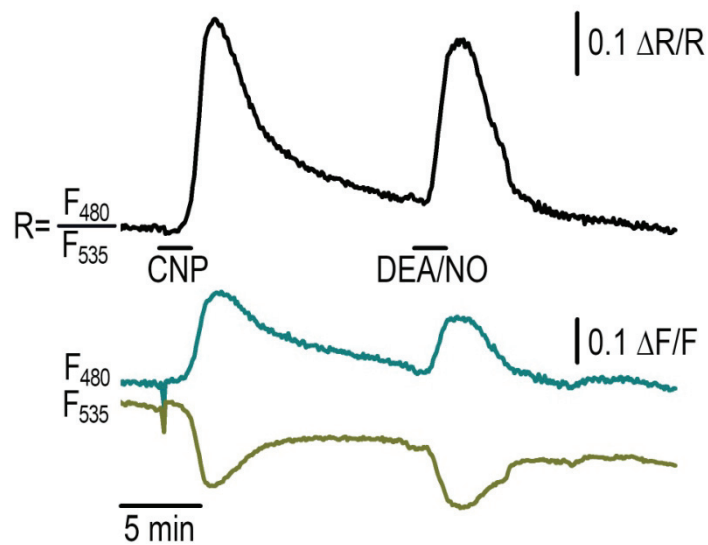
Online Figure I. Generation of SM22-cGi500 mice. **A**, The SM22-cGi500 transgene consists of a 445-bp fragment of the murine SM22 α gene promoter (P_{SM445}) followed by a rabbit β -globin intron, the cGi500 coding sequence, and two polyadenylation signals (white boxes) derived from the rabbit β -globin gene and SV40. **B**, Western Blot analysis of tissue extracts (4 μ g) from transgenic mice (tg/+) and non-transgenic control animals (+/+) with an antiserum against EGFP to detect cGi500 protein; GAPDH was used as a loading control. **C**, Live YFP fluorescence of the smooth muscle layer of the bladder (left) and colon (right). Scale bars, 100 μ m. **D**, Primary VSMCs, BSMCs, and CSMCs from SM22-cGi500 mice were analyzed for live YFP fluorescence (upper panels) or by immunofluorescence staining with antibodies against EGFP (green) and SM22 α (red); cell nuclei were stained with Hoechst 33258 (blue). Scale bars, 100 μ m.



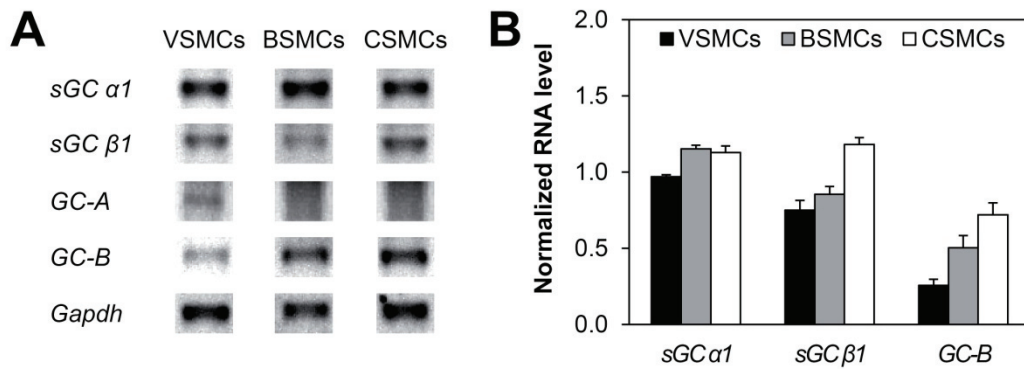
Online Figure II. Generation of R26-CAG-cGi500 mice. **A**, Schematic diagram of the gene targeting strategy to insert a Cre-activatable cGi500 construct into the intron between exon 1 and 2 (grey boxes) of the murine ROSA26 locus (+ allele). The targeting construct contained the CAG promoter (P_{CAG}) driving the expression of a loxP-flanked (black arrowheads) membrane-targeted tandem-dimer Tomato (mT, red) and of cGi500 (green) before and after Cre-mediated recombination, respectively. Expression cassettes encoding a FRT-flanked (white arrowheads) neomycin resistance gene (Neo) and diphtheria toxin A (DTA) were used for positive and negative selection of ES cell clones. Integration of the targeting construct via homologous recombination results in a “L2 allele” with two loxP sites, and Cre-mediated excision of mT results in a “L1 allele” with one loxP site. Also indicated are EcoRV restriction sites (EV), the probe and DNA fragments used for Southern blot analysis of ES cell clones as well as the primers (half arrows) used for PCR genotyping of mice. Primers P1, P2, P3 in the figure correspond to primers ROSA10, ROSA11, ROSA4 in the methods section, respectively. **B**, Southern blot of EcoRV-digested genomic DNA of wild-type (+/+), targeted (+/L2) and Cre-recombined (+/L1) ES cell clones. The expected positions of the DNA fragments derived from the respective alleles are indicated to the left.



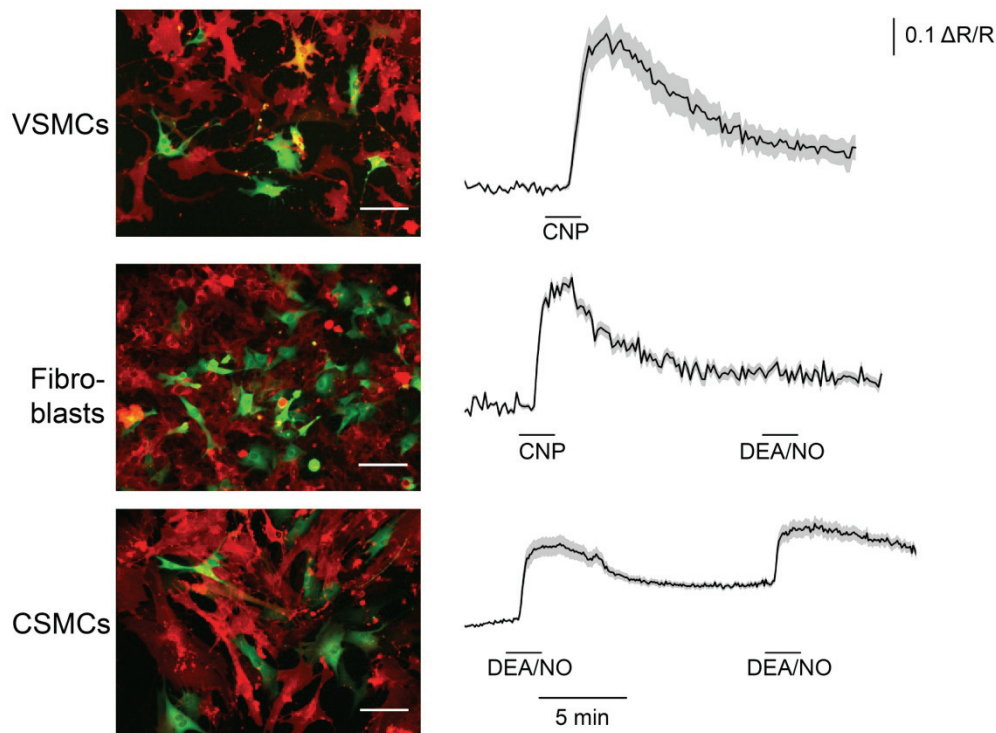
Online Figure III. Global expression of cGi500 in R26-CAG-cGi500(L1) mice. Sensor fluorescence was detected using a EGFP or YFP filter set in **(A)** unfixed whole mounts (upper) and fixed cryosections (lower) of various organs from a 6-week-old transgenic mouse, **(B)** transgenic embryos (12.5 dpc), and **(C)** primary aortic VSMCs or **(D)** fibroblasts from adult animals. Stars indicate the positions of control samples from non-transgenic littermates. Scale bars, 100 μ m.



Online Figure IV. cGMP FRET in primary VSMCs from R26-CAG-cGi500(L1) mice. Cells were analyzed under similar conditions as primary VSMCs from SM22-cGi500 mice (see Figure 1C). Short stimulations (2 min) with CNP (50 nM) or DEA/NO (100 nM) lead to reversible cGMP increases. Cyan, yellow and black traces indicate CFP emission (F_{480}), YFP emission (F_{535}) and the CFP/YFP emission ratio (F_{480}/F_{535}), respectively. Emission intensities and ratios were normalized to averaged baseline signals and are given as $\Delta F/F$ and $\Delta R/R$, respectively. One representative recording out of four experiments is shown.



Online Figure V. Analysis of guanylyl cyclase expression by semi-quantitative RT-PCR. RNA was extracted from VSMCs, BSMCs, and CSMCs isolated from SM22-cGi500 mice. Reverse transcription was performed with 250 ng total RNA using gene-specific primers. PCR reactions were performed with 1/10 of the cDNA and aliquots were taken every third cycle between cycle 25 and 40. **A**, PCR products obtained for *sGC α1* (cycle 37), *sGC β1* (cycle 40), *GC-A* (cycle 40), *GC-B* (cycle 40), and *Gapdh* (cycle 34). **B**, For densitometric evaluation, band intensities of 3 consecutive aliquots were normalized to *Gapdh*. Shown are mean values ± s.e.m. of 3 cycles. Note that *GC-A* mRNA was not quantified, because it was detected only in VSMCs. RT-PCR analysis of *GC-A* and *GC-B* was repeated with 500 ng total RNA and random hexamer/polyT primers and similar results were obtained.



Online Figure VI. Validation of cells from R26-CAG-cGi500(L2) mice. VSMCs, fibroblasts, and CSMCs were isolated from R26-CAG-cGi500(L2) mice and then transfected by lipofection with a Cre-expressing plasmid. The detection of green fluorescent cells confirmed that Cre-mediated excision of the mT sequence (encoding a membrane-tagged red fluorescent protein, Online Figure IIA) enables cGi500 expression in all analyzed cell types (left panels). To test the functionality of the cGi500-positive cells, FRET imaging was performed (right panels). Cells were stimulated with CNP or DEA/NO (VSMCs with 50 nM CNP, fibroblasts with 100 nM CNP followed by 100 nM DEA/NO, and CSMCs two times with 100 nM DEA/NO). Data shown are mean \pm s.e.m.. The number of analyzed VSMCs, fibroblasts, and CSMCs was 8, 10, and 8, respectively. Scale bars, 100 μ m.